

## Interface locking along the subduction megathrust from $b$ -value mapping near Nicoya Peninsula, Costa Rica

Abhijit Ghosh,<sup>1,2</sup> Andrew V. Newman,<sup>1</sup> Amanda M. Thomas,<sup>1,3</sup> and Grant T. Farmer<sup>1</sup>

Received 7 August 2007; revised 7 October 2007; accepted 9 November 2007; published 1 January 2008.

[1] To understand controlling factors for seismogenesis and strain-accumulation in subduction megathrusts we examine seismicity patterns across Nicoya, Costa Rica, to determine the overall and spatial variability in the earthquake frequency-magnitude distribution along the interface. The mean reduction in earthquake activity with magnitude,  $b$ -value, is higher (1.06) than global subduction zone averages (0.6–0.8), suggesting the interface here is weakly coupled. Strong spatial variations in  $b$  are anticorrelated (–0.53) with geodetic estimates of interface locking of E. Norabuena et al. (2004). High  $b$  prevails in two regions, including the subducted Fisher seamount chain. A broad zone of reduced  $b$  is observed at and offshore the central Nicoya coast; extending towards an imaged locked patch. These results suggest  $b$ -value studies may be useful in identifying regions of increased interface locking in subduction zones, which may indicate regions capable of large slip in future large earthquakes.  
**Citation:** Ghosh, A., A. V. Newman, A. M. Thomas, and G. T. Farmer (2008), Interface locking along the subduction megathrust from  $b$ -value mapping near Nicoya Peninsula, Costa Rica, *Geophys. Res. Lett.*, 35, L01301, doi:10.1029/2007GL031617.

### 1. Introduction

[2] The majority of the world's largest earthquakes are generated at the plate interface of subduction zone megathrusts, thus it is important to understand which processes here are responsible for the development of earthquake potential. While it is generally assumed that large earthquakes at the plate interface are the result of stick-slip behavior, we do not clearly understand the physical processes that control the onset and termination of zones that exhibit this behavior, and whether the behavior remains consistent over the seismic cycle. One of the largest difficulties in accurately constraining the seismogenic extent of subduction zones is that most subduction megathrusts occur almost entirely offshore, thus making it difficult for land-based techniques to detect microseismicity. However, because the Nicoya Peninsula of Costa Rica extends the shoreline significantly closer to the trench, this region is uniquely situated to proximally examine interface seismicity along the megathrust, hereafter seismogenic

zone, using primarily land-based techniques (Figure 1). To take advantage of this geometry, the Costa Rica Seismogenic Zone Project (CRSEIZE) was performed by UC Santa Cruz, Observatorio Volcanológico y Sismológico de Costa Rica, University of Miami, and UC San Diego, and was able to capture much of the ongoing earthquake activity and deformation due to seismogenic zone processes (Figure 1) [Newman et al., 2002; DeShon and Schwartz, 2004; Norabuena et al., 2004; DeShon et al., 2006]. The experiment ran in Nicoya Peninsula between late-1999 and mid-2001 with a combined 20 station on-land broad-band and short-period network. For the 1st six months, the network was augmented by a 14 station offshore ocean-bottom deployment forming a transect between the Nicoya shoreline and the down-going Cocos plate crossing the Middle America Trench (MAT).

[3] Using data collected during the CRSEIZE experiment, we spatially map the frequency-magnitude distribution (FMD) of earthquakes. We use the resultant interface information to determine its utility for detecting coupling along the seismogenic zone beneath Nicoya. The FMD of earthquakes, which was first introduced by Ishimoto and Iida [1939] and Gutenberg and Richter [1944], has a power-law relationship, such that

$$\log_{10} N = a - bM,$$

where  $N$  is the cumulative number of earthquakes greater than or equal to magnitude  $M$ , and  $a$  and  $b$  are constants describing the activity and slope, respectively. Here, we focus on the parameter  $b$ , or  $b$ -value, which describes the ratio of occurrence of small to large earthquakes. Globally,  $b$ -value is  $\sim 1$  [e.g., Stein and Wysession, 2003], meaning a 10-fold decrease in seismic activity occurs with each subsequent unit magnitude increase. However,  $b$  is observed to vary between individual fault zones [e.g., Wesnousky, 1994; Schorlemmer and Wiemer, 2005], and even within a particular space and time range [e.g., Nuannin et al., 2005]. Though several attempts were made to understand the physical meaning of  $b$ , a conclusive answer remains elusive. Both laboratory experiments of material behavior [Mogi, 1962; Scholz, 1968; Warren and Latham, 1970; Wyss, 1973; Amitrano, 2003], and field surveys of earthquakes along faults [Schorlemmer and Wiemer, 2005] suggest that  $b$ -values reflect the stress regime along the body or fault—the lower the  $b$ -value, the higher the stress. More recently, Schorlemmer et al. [2005] used both global and regional earthquake catalogs to show that the  $b$ -value acts as stress meter that depends inversely on differential stress.

[4] In the subduction zones,  $b$ -value studies have been mostly limited to identifying the extent of magmagenesis

<sup>1</sup>School of Earth and Atmospheric Sciences, Georgia Institute of Technology, Atlanta, Georgia, USA.

<sup>2</sup>Now at Department of Earth and Space Sciences, University of Washington, Seattle, Washington, USA.

<sup>3</sup>Now at Department of Earth and Planetary Science, University of California, Berkeley, California, USA.

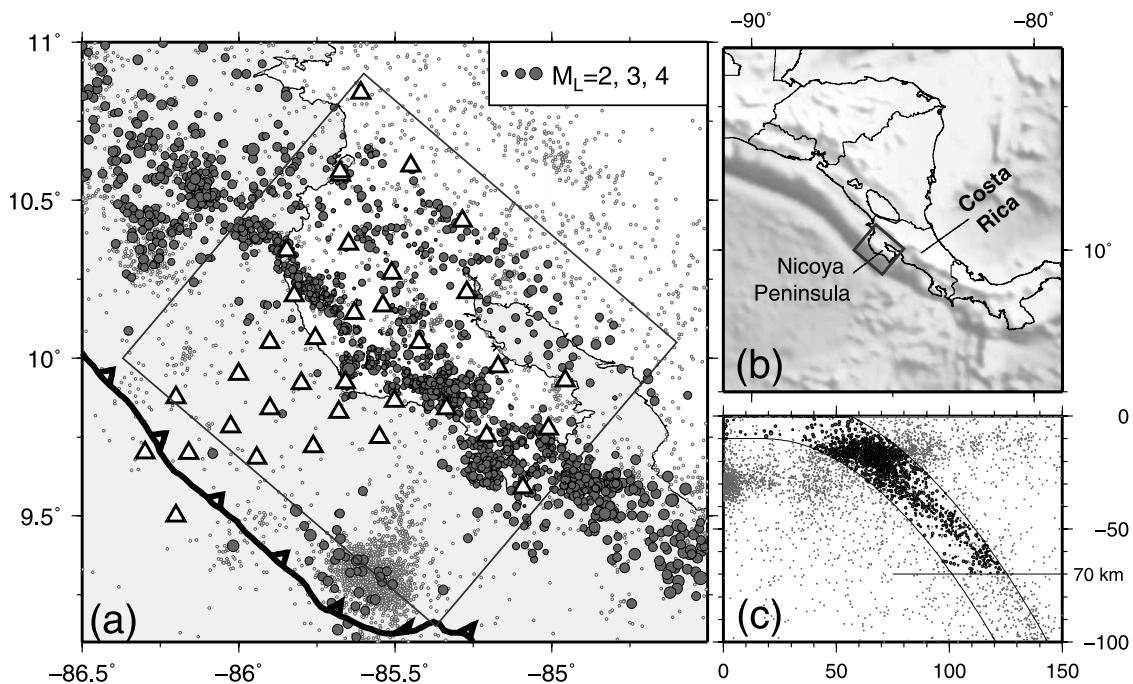


**Figure 1.** (a) Seismicity recorded over the Nicoya Peninsula of Costa Rica (b) by the CRSEIZE network (open triangles). Scaled darkened earthquakes in map view (Figure 1a) and (c) cross section are a subset of the total low error catalog (open circles) used in this study. A saw-toothed curve represents the Middle America Trench. The boxed area in Figures 1a and 1b is the focus data region for the remainder of the study. Thin lines in Figure 1c show the parabolic and depth boundaries of the utilized data set.

associated with arc volcanism [Wiemer and Benoit, 1996; Monterroso and Kalháněk, 2003] because most seismicity catalogs of activity along the plate interface are insufficient for detailed analysis. However, in a fault interface study along the Parkfield section of the San Andreas Fault, a continental transform, Schorlemmer and Wiemer [2005] found that areas of low  $b$  contained most of the slip and aftershocks of the 2004  $M_w$  6.0 earthquake. This result suggests that  $b$  may not be static along an individual fault, but may change over the seismic cycle, and is lowest in regions with increased strain energy before a large earthquake [Schorlemmer and Wiemer, 2005].

## 2. Tectonic Setting

[5] In Costa Rica, the MAT is characterized by the subduction of oceanic Cocos plate beneath the overriding Caribbean plate (Figure 1) at a rate of 8–9 cm/yr [DeMets, 2001]. Interestingly, the down-going Cocos plate beneath Nicoya is comprised of sea floor from two origins, of similar age. The northern section is generated at the fast-spreading East Pacific Rise (EPR), while the medium-spreading Cocos-Nazca Spreading Center (CNS) crust subducts beneath southern Nicoya [Barckhausen et al., 2001]. Using data collected from CRSEIZE, Newman et al. [2002] identified a 5-km upward shift in shallow interface seismicity at the transition from EPR to CNS crust near 10°N, coincident with an abrupt change in oceanic plate heat flow with the EPR being significantly cooled [Harris and Wang, 2002; Fisher et al., 2003]. Changes in the geometry and thermal parameters of the

subducting plate interface may contribute to heterogeneous coupling across the region.

## 3. Data and Methodology

[6] We use existing earthquake phase timing and seismic waveform data spanning the Nicoya portion of CRSEIZE to develop a nearly “complete” record of seismicity beneath Nicoya between late-1999 and mid-2001. While ~5000 events from CRSEIZE were determined and subsets used by DeShon et al. [2006] and earlier studies, it was necessary to manually identify another ~5000 events, and determine local magnitudes ( $M_L$ ) in order to develop a consistent and robust catalog. Using the catalog of over 10,000 earthquakes we relocated the events within local three dimensional  $V_P$  and  $V_P/V_S$  velocity models of DeShon et al. [2006], using the methodology explained by Newman et al. [2002]. Because of spatial limitations in the DeShon velocity model and differences in location algorithms, about 10% of the events did not converge, resulting in a data set of 8717 regional earthquakes (open circles in Figure 1). From the resulting data set we retain only events with formal epicentral location errors of less than 5 km (~200 removed), are shallower than 70 km depth, and within 10 km of a best fit parabolic function that describes interface and slab seismicity (~5800 removed; Figure 1c). By doing so, we eliminate most poorly located and crustal events that are not associated with plate-interface activity. Because a temporally consistent catalog is necessary for  $b$ -value analysis, we remove a period between July 21 and Sept. 16, 2000, due to significant aftershock activity from the July 21  $M_w$  6.4 Nicoya outer-rise earthquake (286 removed) [Newman et

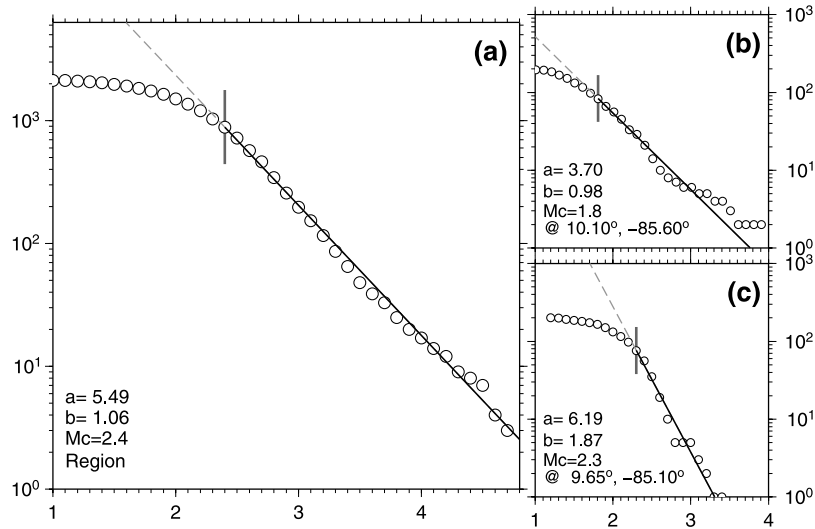


**Figure 2.** The frequency-magnitude distribution for the (a) boxed seismicity in Figure 1 and individual grid nodes in (b) low and (c) high  $b$ -value zones (isolated nodes shown in Figure 3). For each, the maximum likelihood best fit solution (thin diagonal lines) and magnitude of completeness  $M_C$  (short vertical line) are shown.

*et al.*, 2002]. For the remainder of this paper, we describe results only using this catalog of 2428 well-located events approximating the megathrust interface in this region (solid circles in Figure 1).

[7] From this catalog we perform FMD mapping using algorithms similar to ZMAP [Wiemer, 2001]. We determine the magnitude of completeness ( $M_C$ ) for the overall catalog and over a  $0.025^\circ \times 0.025^\circ$  horizontal grid. We determine an initial  $M_C$  from the maximum curvature method [Wiemer and Wyss, 2000], and use the value as an initial value to determine a new  $M_C$  minimizing the misfit between the data and synthetics [Wiemer and Wyss, 2000]. Using this method we determine the overall  $M_C$  is 2.4 (Figure 2a), however the value varies spatially between 1.5 and 2.9. Because there are significant variations in  $M_C$ , we choose to calculate  $M_C$  in each grid node and eliminate all the events below it, rather than using an averaged constant  $M_C$ . Doing so reduces bias in  $b$ -value calculations in regions with  $M_C$  higher than the regional average.

[8] Within our region of interest, we sample the closest 200 events in a vertical cylindrical volume around each node, and used the maximum likelihood method [Aki, 1965] to calculate the local  $b$ -value from events greater than  $M_C$ . Likewise, we define a maximum useful sampling radius of 35 km to negate nodes that have severely smoothed data. Because we require a large number of events per analysis and are imaging these results at a fine scale, neighboring results within the scale of the sampling radius are not independent. However, the finer  $0.025^\circ$  grid spacing was chosen to improve observations of changes in the variability of  $b$ .

#### 4. Results and Discussion

[9] The overall  $b$ -value for the subset catalog is found to be  $1.06 \pm 0.034$  ( $1\sigma$ ; Figure 2), which is higher than the published subduction zone average ( $b \sim 0.5$  to  $0.8$ ) [Bayrak

*et al.*, 2002], indicating a mostly weak megathrust interface below Nicoya. However, the most striking feature is the spatial variability along the interface (Figures 2b, 2c, and 3). Interface  $b$ -values range from 0.8 to more than 2.0 within the region, with the lowest pronounced zone near central Nicoya Peninsula, and bounded on both ends by zones with higher values. While  $b$ -values significantly above 2 are generally considered extreme, and a potential sign of systematic overestimation of smaller events, we consider this possibility unlikely since magnitudes are determined using a homogeneous seismic network and measured across a similar crustal structure. Examples of  $b$ -value and  $M_C$  determinations for two nodes are shown in Figures 2b and 2c, and their positions are identified in Figure 3. As a test of our algorithms, we repeat the FMD mapping on the same data set using ZMAP, and least-squares regression for  $b$ , both of which yielded similar patterns and values of spatial variability. For most of the region of interest solutions have errors that are less than 20% of the associated  $b$ -values, as determined using a bootstrap of 10,000 random distributions of earthquakes for each grid sample (Figure 3b). Errors are comparable, but on average 4% higher than the method described by Shi and Bolt [1982].

[10] Previous work in earthquake FMD has shown that  $b$ -values reflect the overall stress regime [Scholz, 1968; Wyss, 1973] with fluctuations in differential stress as the most important factor that affects  $b$  [Schorlemmer *et al.*, 2005]. While it has been argued that material heterogeneity and temperature can also affect  $b$ -values [Mogi, 1962; Warren and Latham, 1970], it is not clear that their affects are independent of their associated changes in stresses. Additionally, it is suggested that neither material heterogeneity nor temperature significantly affect  $b$ -values in subduction zones [Wiemer and Benoit, 1996]. Thus, we propose that the low  $b$ -value region indicates an area of high differential-stress accumulation along the seismogenic interface beneath Nicoya.

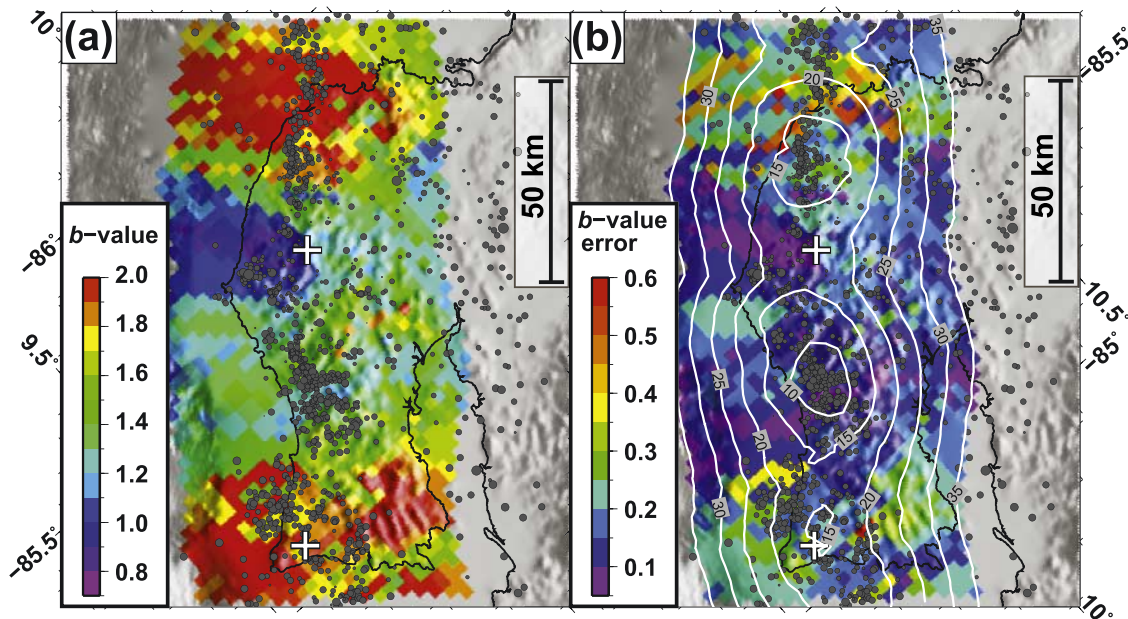


**Figure 3.** (a) Spatial variations in  $b$ -values. (b) Results are retained for nodes with sampling radius (white contours) less than 35 km. Additionally, errors determined using the bootstrap method are shown ( $1\sigma$ ). White crosses show isolated nodes whose  $b$ -value determinations are shown in Figure 2.

[11] The low  $b$ -value zone coincides with a transition between EPR and CNS oceanic crust [Barckhausen *et al.*, 2001], and an irregular subducted surface [Newman *et al.*, 2002; DeShon *et al.*, 2006]. While at present we do not have resolution to determine details of interface locking using  $b$ -value mapping, it may be controlled partially by the roughness along the CNS-EPR boundary and an already subducted segment of the Fisher seamount chain, causing additional roughness that perturbs the stress field along the interface. Analogous data from the San Andreas fault shows similarly locked portions of the fault having significantly reduced  $b$  than the adjacent creeping section [Amelung and King, 1997; Schorlemmer *et al.*, 2004]. We contend that variations in interface topography may be affecting the distribution of locking, and hence the  $b$ -values along the interface.

[12] Our interpretation is independently supported by a geodetic study which found an increase in locking in central Nicoya, using GPS deformation data collected between 1994 and 2000 [Norabuena *et al.*, 2004]. The model-derived locked subduction interface corresponds with a broad low  $b$ -value zone located at and offshore central Nicoya in this study (Figure 4). It should be understood that because most earthquake activity occurs downdip of this region, the  $b$ -values determined offshore become increasingly spatially biased by downdip seismicity. However, the lack of significant seismicity along the updip interface is itself, associated with increased coupling, suggesting that this portion of the interface is more strongly locked.

[13] Regions of high  $b$  correspond with geodetically modeled weak patches over the down-dip extension of the Fisher seamounts, in a portion of the interface imaged as having a subducted seamount [Husen *et al.*, 2003], further suggesting such subducted topography perturbs the stress-field along the interface. Directly comparing values of  $b$  taken every 10 km with locking along the geodetically

modeled interface we find a moderate negative correlation ( $-0.53$ ), with high scatter (Figure 4). This result indicates that  $b$ -values are inversely affected by the degree of locking along a fault plane. Testing with 10,000 randomly generated data sets of the same sample size ( $n = 30$ ), we found that the possibility of a correlation of at least  $|\cdot 53|$  occurring from purely random sampling can be excluded at 99.6% confidence. While the correlation between these data types does appear real, the strength of the correlation is likely reduced by a number of factors, including (a) different periods of measurement, (b) noise in data sets, (c) assumptions required by geodetic modeling (e.g., homogenous elastic strength and simplified geometry), (d) differences in spatial sampling and smoothing between geodetic and FMD methods, and (e) relationship between locking and  $b$  may not be linear.

## 5. Conclusions

[14] Significant spatial variation in  $b$ -values are found along MAT interface near Nicoya Peninsula. The overall  $b$  suggests a weakly coupled subduction interface in the study area, however a region of lower  $b$ -values is detected in central Nicoya that suggests a region of increased differential stress, hence locking along the megathrust. This interpretation is corroborated by an independent geodetic study. While inversion of the geodetic data may be optimal for determining the overall interface locking, the results have significantly smoothed (dependent on station spacing and locking depth), and require assumptions about material homogeneity and precise slab geometry. Alternatively, mapping seismic  $b$ -values require fewer assumptions and can help constrain locking in regions that are not easily accessible by land-based geodetic techniques, such as the updip regions of most subduction zone environments. This work

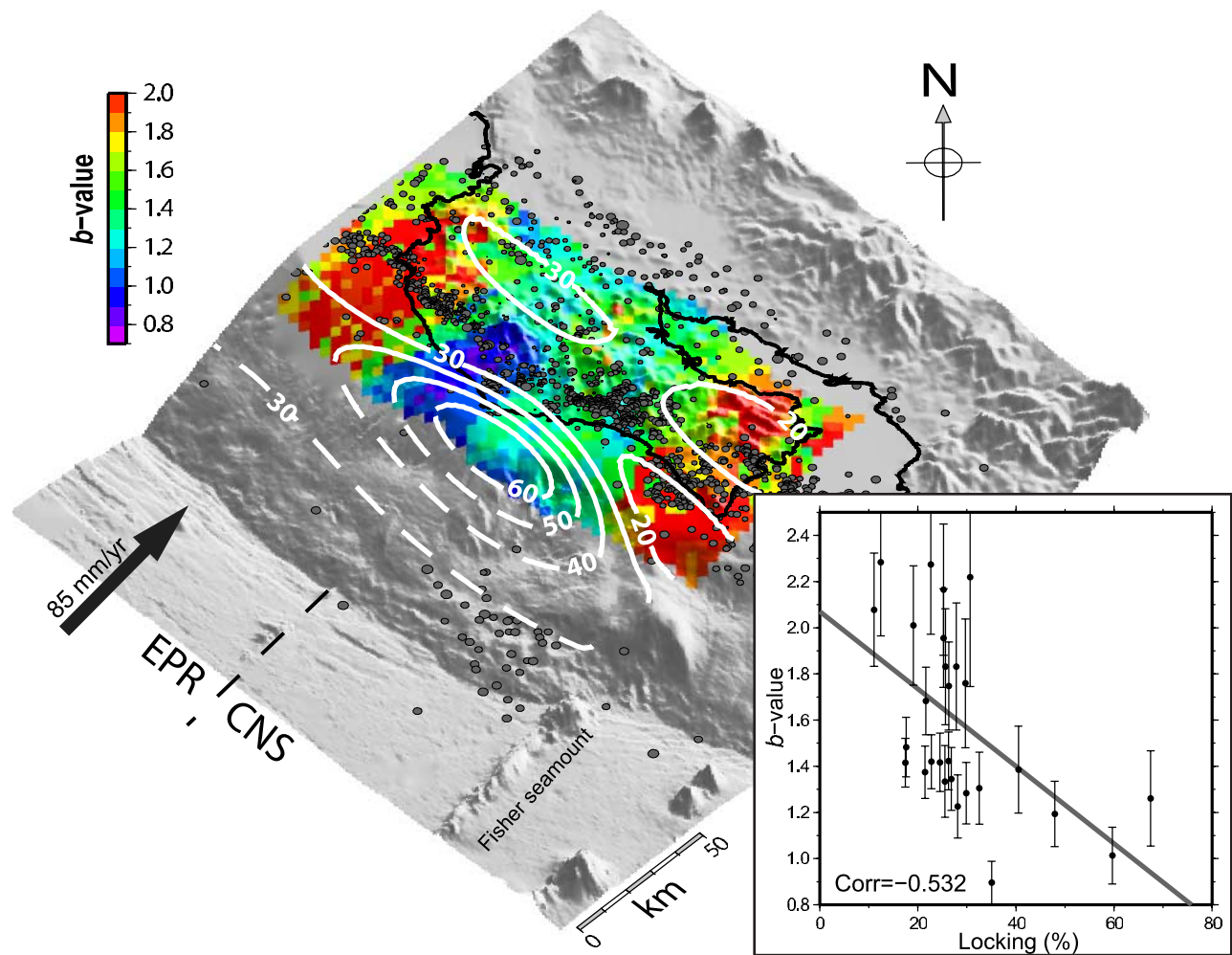


**Figure 4.** Geodetically determined locking from *Norabuena et al.* [2004] is shown (white contours) with variations in  $b$  from Figure 3 and interface seismicity (dark circles). More poorly constrained geodetic results are shown as a dashed line. High resolution bathymetry [*Ranero and von Huene, 2000*] shows the Fisher seamount chain, which is subducting nearly trench-normal at  $\sim 85$  mm/yr [*DeMets, 2001*] and coincident with undulations in locking and high  $b$ -values. Transition between East Pacific Rise (EPR) and Cocos-Nazca Spreading Center (CNS) oceanic crust is also shown. (inset) A comparison of  $b$  and locking shows negative correlation ( $-0.532$ ) suggesting  $b$  varies inversely with locking. Line fit is  $y(x) = 2.1 - 0.017x$ .

finds that spatial  $b$ -value mapping of the subduction zone interface is effective, if adequate seismic data exist.

[15] **Acknowledgments.** We thank for prior and recent earthquake analyses (by analysts including J. Convers and A. Koerner) and for the thoughtful advice and reviews from Z. Peng, S. Bilek, S. Nakaya, and an anonymous reviewer. Thanks to Jana Stankova-Pursley for helping us in developing the parabolic function for the interface. Figures were developed using GMT [*Wessel and Smith, 1998*]. NSF grant OCE-9910609 supported CRSEIZE, and Georgia Tech Research Foundation supported this study.

## References

- Aki, K. (1965), Maximum likelihood estimate of  $b$  in the formula  $\log_{10} N = a - bM$  and its confidence limits, *Bull. Earthquake Res. Inst. Univ. Tokyo*, *43*, 237–239.
- Amelung, F., and G. King (1997), The difference between earthquake scaling laws for creeping and non-creeping faults, *Geophys. Res. Lett.*, *24*, 507–510.
- Amitrano, D. (2003), Brittle-ductile transition and associated seismicity: Experimental and numerical studies and relationship with the  $b$ -value, *J. Geophys. Res.*, *108*(B1), 2044, doi:10.1029/2001JB000680.
- Barckhausen, U., C. R. Ranero, R. von Huene, S. C. Cande, and H. A. Roeser (2001), Revised tectonic boundaries in the Cocos plate off Costa Rica: Implications for the segmentation of the convergent margin and for plate tectonic models, *J. Geophys. Res.*, *106*, 19,207–19,220.
- Bayrak, Y., A. Yılmaztürk, and S. Öztürk (2002), Lateral variation of the modal ( $a/b$ ) values for the different regions of the world, *J. Geodyn.*, *34*, 653–666.
- DeMets, C. (2001), A new estimate for Cocos-Caribbean plate motion: Implications for slip along the Central American volcanic arc, *Geophys. Res. Lett.*, *28*, 4043–4046.
- DeShon, H. R., and S. Y. Schwartz (2004), Evidence for serpentinization of the forearc mantle wedge along the Nicoya Peninsula, Costa Rica, *Geophys. Res. Lett.*, *31*, L21611, doi:10.1029/2004GL021179.
- DeShon, H. R., S. Y. Schwartz, L. M. Dorman, A. V. Newman, V. Gonalaz, M. Protti, T. Dixon, E. Norabuena, and E. Flueh (2006), Seismogenic zone structure along the Middle America Trench, Nicoya Peninsula, Costa Rica, from 3D local earthquake tomography using  $P$ - and  $S$ -wave data, *Geophys. J. Int.*, *164*, 109–124.
- Fisher, A. T., C. A. Stein, R. N. Harris, K. Wang, E. A. Silver, M. Pfender, M. Hutnak, A. Cherkaoui, R. Bodzin, and H. Villinger (2003), Abrupt thermal transition reveals hydrothermal boundary and role of seamounts within the Cocos plate, *Geophys. Res. Lett.*, *30*(11), 1550, doi:10.1029/2002GL016766.

- Gutenberg, B., and C. F. Richter (1944), Frequency of earthquakes in California, *Bull. Seismol. Soc. Am.*, *34*, 185–188.
- Harris, R., and K. Wang (2002), Thermal models of the Middle America Trench at the Nicoya Peninsula, Costa Rica, *Geophys. Res. Lett.*, *29*(21), 2010, doi:10.1029/2002GL015406.
- Husen, S., R. Quintero, E. Kissling, and B. Hacker (2003), Subduction-zone structure and magmatic processes beneath Costa Rica constrained by local earthquake tomography and petrological modeling, *Geophys. J. Int.*, *155*, 11–32, doi:10.1046/j.1365-246X.2003.01984.
- Ishimoto, M., and K. Iida (1939), Observations of earthquakes registered with the microseismograph constructed recently, *Bull. Earthquake Res. Inst. Univ. Tokyo*, *17*, 443–478.
- Mogi, K. (1962), Magnitude-frequency relations for elastic shocks accompanying fractures of various materials and some related problems in earthquakes, *Bull. Earthquake Res. Inst. Univ. Tokyo*, *40*, 831–853.
- Monteroso, D. A., and O. Káhlánek (2003), Spatial variation of  $b$ -values in the subduction zone of Central America, *Geofis. Int.*, *42*, 575–587.
- Newman, A. V., S. Y. Schwartz, V. Gonzalez, H. DeShon, J. Protti, and L. M. Dorman (2002), Along-strike variability in the seismogenic zone below Nicoya Peninsula, Costa Rica, *Geophys. Res. Lett.*, *29*(20), 1977, doi:10.1029/2002GL015409.
- Norabuena, E., et al. (2004), Geodetic and seismic constraints on some seismogenic zone processes in Costa Rica, *J. Geophys. Res.*, *109*, B11403, doi:10.1029/2003JB002931.
- Nuannin, P., O. Kulhanek, and L. Persson (2005), Spatial and temporal  $b$ -value anomalies preceding the devastating off coast of NW Sumatra earthquake of December 26, 2004, *Geophys. Res. Lett.*, *32*, L11307, doi:10.1029/2005GL022679.
- Ranero, C. R., and R. von Huene (2000), Subduction erosion along the Middle America convergent margin, *Nature*, *404*, 748–752.
- Scholz, C. H. (1968), The frequency-magnitude relation of microfracturing in rock and its relation to earthquakes, *Bull. Seismol. Soc. Am.*, *58*, 399–415.
- Schorlemmer, D., and S. Wiemer (2005), Microseismicity data forecast rupture area, *Nature*, *434*, 1086, doi:10.1038/4341086a.
- Schorlemmer, D., S. Wiemer, and M. Wyss (2004), Earthquake statistics at Parkfield: 1. Stationarity of  $b$ -values, *J. Geophys. Res.*, *109*, B12307, doi:10.1029/2004JB003234.
- Schorlemmer, D., S. Wiemer, and M. Wyss (2005), Variation in earthquake-size distribution across different stress regimes, *Nature*, *437*, 539–542, doi:10.1038/nature04094.
- Shi, Y., and B. A. Bolt (1982), The standard error of the magnitude-frequency  $b$  value, *Bull. Seismol. Soc. Am.*, *72*, 1677–1687.
- Stein, S., and M. Wysession (2003), *An Introduction to Seismology, Earthquakes, and Earth Structure*, Blackwell, Oxford, U. K.
- Warren, N. W., and G. Latham (1970), An experiment study of thermal induced micro-fracturing and its relation to volcanic seismicity, *J. Geophys. Res.*, *75*, 4455–4464.
- Wesnousky, S. G. (1994), The Gutenberg-Richter or characteristic earthquake distribution, which is it?, *Bull. Seismol. Soc. Am.*, *84*, 1940–1959.
- Wessel, P., and W. H. F. Smith (1998), New, improved version of generic mapping tools released, *Eos Trans. AGU*, *79*, 579.
- Wiemer, S. (2001), A software package to analyze seismicity: ZMAP, *Seismol. Res. Lett.*, *72*, 373–382.
- Wiemer, S., and J. P. Benoit (1996), Mapping the  $b$ -value anomaly at 100 km depth in the Alaska and New Zealand subduction zones, *Geophys. Res. Lett.*, *23*, 1557–1560.
- Wiemer, S., and M. Wyss (2000), Minimum magnitude of completeness in earthquake catalogues: Examples from Alaska, the western United States, and Japan, *Bull. Seismol. Soc. Am.*, *90*, 859–869.
- Wyss, M. (1973), Towards a physical understanding of the earthquake frequency distribution, *Geophys. J. R. Astron. Soc.*, *31*, 341–359.

---

G. T. Farmer and A. V. Newman, School of Earth and Atmospheric Sciences, Georgia Institute of Technology, Atlanta, GA 30331, USA. (anewman@gatech.edu)

A. Ghosh, Department of Earth and Space Sciences, University of Washington, Seattle, WA 98195-1310, USA.

A. M. Thomas, Department of Earth and Planetary Science, University of California, Berkeley, Berkeley, CA 94720-4767, USA.